Korean J. Chem. Eng., 37(5), 766-775 (2020)
DOI: 10.1007/s11814-020-0495-4

pISSN: 0256-1115
eISSN: 1975-7220

Adsorption of phosphate from aqueous solution by lanthanum modified macroporous chelating resin

Xiaoting Zhang, Chenghui Ma, Kang Wen, and Runping Han†

College of Chemistry, Zhengzhou University, No 100 of Kexue Road, Zhengzhou, 450001, P. R. China
(*Received 19 September 2019 • accepted 18 January 2020*)

Abstract−A highly effective adsorbent of lanthanum-modified D751 resin (D751 resin for macroporous styrene chelated resin, sodium form) was prepared to enhance the effect of removing phosphate from solution. FTIR, SEM were used to explore the functional groups and structural features on the surface of D751-La; XPS analyzed the action mechanism between phosphate and D751-La. The adsorption performance about D751-La toward phosphate was investigated by batch experiment. The results showed that Langmuir, Freundlich, Temkin, Koble-Corrigan as well as Redlich-Peterson models fitted well for the adsorption isotherms. The adsorption kinetics could be better fitted by Double Constant, Elovich, and Pseudo-second-order model. The effect of salinity was not significant, such as Cl^- and SO_4^{2-}. When the solid-liquid ratio was 15 g·L^{-1} with setting the reaction time as 8 h, the unit adsorption quantity of D751-La to phosphate (calculated in P) reached up to 26.3 mg·g^{-1} under the solution pH=3 at 293 K. The process was spontaneous and exothermic from thermodynamic analysis. It shows that D751-La has potential to remove phosphate from solution.

Keywords: Phosphate, Lanthanum-modified D751 Resin, Adsorption

INTRODUCTION

As a nutrient element, phosphorus is very essential for the healthy growth of all plants and animals [1,2]. However, phosphorus-containing wastewater, which is usually produced by arbitrary discharge without permission of factory wastewater and domestic sewage, has become the main reason for the eutrophication of water bodies. The extensive use of phosphorus-containing fertilizers and pesticides seriously harms the self-purification function of the water body [3-6]. Finding an efficient and economical method for removal of phosphorus is imminent [7].

At present, there are many technical means for phosphorus removal, mainly including chemical precipitation, ion exchange, electrodialysis, biological method and adsorption technique [8]. However, there are still defects in these methods, such as the exchange capacity about objects significantly decreases with the increase of salt concentration. Biological method for removal of phosphorus is currently more economical, but the excess sludge generated in the process needs further treatment to prevent secondary pollution, and the effect of several factors is unstable. In the chemical precipitation method, metal salt is mostly used for phosphorus removal, and metal ions left in the phosphorus removal process also cause secondary pollution to the environment [9]. The ion exchange method has some limitations in certain aspects [10]. Electrodialysis is costly, difficult to control, and is not available to use in the treatment of large amounts of wastewater. However, the adsorption method with some advantages, such as high adsorption, simple operation, low cost without pollution again, has been used by more and more for phosphorus removal [11]. For example, Savic et al. used magnetite-coated tuff grains to remove phosphate and found that the maximum adsorption capacity toward phosphate upon magnetite-coated tuff grains was 1.91 mg·g^{-1} [12]. Afridi et al., who explored the effect of anodized iron oxide nanoflakes on phosphate adsorption, revealed that the maximum adsorption capacity was only 21.45 mg·g^{-1} for phosphate [9]. However, the mass adsorbents for removing phosphate in these studies are still not ideal. In the face of severe eutrophication, it is quite important to find a method to significantly increase the amount of phosphorus adsorption, which has been paid more and more attention. In addition to the above advantages, the resin as the adsorbent has the characteristics of high degree of functionalization, large degree of crosslinking, and good selectivity. D751 resin as a macroporous styrene-based chelating resin (functional base: N, N-iminodiacetic acid sodium) has stable characteristics compared with other resins. At present, it is widely used to adsorb cations, such as lithium ions [13]. However, there are fewer reports on phosphate removal by modified D751 resin. This study used it in the research of this subject. The adsorption performance of the modified resin on the contaminants was significantly improved.

As the most common inorganic substance, lanthanum ($LaNO_3$) is regarded as a Lewis acid and can react well with Lewis bases. In addition, it is generally considered non-toxic and harmless, with high selectivity and good adsorption effect. So, it has been used more and more for material modification or loading [14,15]. Therefore, $LaNO_3$ was used to modify D751 resin to enhance adsorption capacity toward phosphate. Subsequently, the original resin and the modified resin were investigated by various characterizations. The adsorption performance of the modified materials toward phosphate was explored by batch experiments and adsorption property was presented. In summary, D751-La has the potential to remove phosphorus from solution.

†To whom correspondence should be addressed.
E-mail: rphan67@zzu.edu.cn

MATERIALS AND METHODS

1. Materials and Instrument

Materials: Lanthanum chloride ($LaCl_3 \cdot 7H_2O$) was obtained from Tianjin Komi Chemical Reagent Co., Ltd.; Anhydrous ethanol (C_2H_5OH) was from Fuchen (Tianjin) Chemical Reagent Co., Ltd.; Hydrochloric acid (HCl) was exported to Yantai Shuangshuang Chemical Co., Ltd.; Sodium hydroxide (NaOH) was from Yantai Shuangshuang Chemical Co., Ltd.; Sodium chloride (NaCl) was from Anhui Suzhou Chemical Reagent Factory; Potassium dihydrogen phosphate (KH_2PO_4) was from Beijing Chemical Plant; D751 resin (macroporous chelating ion exchange resin, sodium form: the granularity: 0.3-1.2 mm ≥95%, the moisture content (Na-type): 57.0%, functional group: - N ($CH_2COONa)_2$) was purchased from Aladdin. The above reagents were all analytical pure; the experimental water was deionized water.

Instrument: the main instruments used in this study are following: The concentration of phosphate was known by making use of UV-visible spectrophotometer (752 Shanghai Hanyu Hengping Instrument Co., Ltd.) with a 1 cm path length at 700 nm (the wavelength corresponding to the maximum absorbance of phosphate) (according to the Beer-Lambert law); the pH of all solutions was known with a precision acidity meter (PHS-3C Shanghai instrument scientific instrument) at room temperature; all reactions were carried out in a constant temperature oscillator (SHZ-82 Changzhou Guohua Electric Co., Ltd.) at constant speed (120 rpm); drying of the material in a constant temperature drying oven (202-V1 Shanghai Experimental Instrument Factory).

2. Preparation of D751-Na and D751-La

The adsorbent was prepared by adjusting on the basis of the existing experiments [16]. A certain amount of resin (about 30 g) was taken and added to absolute ethanol (four times the resin volume) and shaken it in a oscillator at 60 °C for 6 h (for sufficiently removing residual organic matter on the surface of D751). Then it was washed with deionized water until tasteless, and a pretreated resin was obtained, which was designated as D751-Na.

Subsequently, the pretreated resin was placed in 0.04 mol·L^{-1} $LaCl_3$ (four times the resin volume) and shaken in a oscillator with 60 °C for 6 h (in this process, the NaOH of 1.0 mol·L^{-1} was slowly added to adjust the pH until OH^-/La^{3+} (calculated in molar ratio) was 0.6, and the solution was changed three to four times). Finally, the deionized water was used to wash the resin for six times and the resin was put in a constant temperature drying oven for 12 h with 60 °C; the modified resin was obtained, which was recorded as D751-La.

3. Characterization of the Adsorbent

The performance of D751-La and adsorption mechanism of phosphate on D751-La was shown by a series of characterizations. First, the isoelectric point of the adsorbent was measured. 0.03 g of D751-La resin and 20 mL volume of 0.01 mol·L^{-1} NaCl solution with pH_0 range of 2-12 were placed in a series of 50 mL conical flasks, and shaken in a water bath at 30 °C, 120 rpm for 15 h. The acidity meter (PHS-3C Shanghai instrument scientific instrument) measured the pH difference before and after the oscillation at room temperature, which was ΔpH. Then it was plotted with pH_0 and the intersection of the curves was the isoelectric point of the material. The load form of lanthanum was determined by FTIR (PE-1710FTIR American PE Company) with KBr as the salt window and the air as blank. Scanning electron microscopy (SEM, Hitachi Su8020, Japan) was applied to watch the changes of the surface morphology of D751-Na and D751-La. X-ray photoelectron spectroscopy (XPS) (Escalab 250Xi, Thermo Fisher, UK) was utilized to obtain information about the chemical valence, surface chemical composition, and structure which is based on the photoelectric effect.

4. Adsorption Experiments

In this experiment, the adsorption performance of D751-La toward phosphate removal was investigated by batch mode.

A certain amount of D751-La and 20 mL solution of phosphate with a certain concentration (calculated in P) were put into multiple conical flasks (50 mL), then shaken in one water bath with a certain temperature, 120 rpm lasting a certain time, respectively. Some effects of solution pH (1-11), adsorbent dosage (0.01-0.10 g), salinity (0-0.20 mol·L^{-1} NaCl and Na_2SO_4) and adsorption temperature (20, 30, 40 °C) were explored. The pH of phosphate solution was regulated with NaOH and HCl solution while it was monitored at the same time by a pH meter. The concentration of the solution after adsorption was calculated by measuring the absorbance at 700 nm by using molybdenum rhenium anti-spectrophotometry.

The adsorption capacity of phosphate onto unit weight of D751-La and removal percentage was calculated according to the following equations.

$$q_e = \frac{V(c_0 - c_e)}{m} \tag{1}$$

$$p = \frac{c_0 - c_e}{c_0} \times 100\% \tag{2}$$

Among them, q_e is the unit adsorption amount (mg·g^{-1}), V is the solution volume (L), m is the mass of D751-La (g), p is the removal rate (%), and c_0 as well as c_e is the concentration of phosphate before and after adsorption by D751-La (mg·L^{-1}), respectively.

5. Adsorption Kinetics Study

0.03 g of D751-La and 20 ml of solution with different phosphate concentration (30 mg·L^{-1}, 40 mg·L^{-1}, 50 mg·L^{-1}, pH=3) were placed in several conical flasks, and shaken in water bath at 293, 303, 313 K for some time, respectively. Its unit adsorption amount was measured by taking it out at different times.

6. Adsorption Equilibrium Study

Accurate 20 mL of different concentrations of phosphate solution (pH=3) was transferred into conical flasks. Soon afterwards, the D751-La with the mass of 0.03 g was added. Next, the mixture was poured into a water bath at 293, 303 and 313 K with continuous shaking for 8 h, respectively. Then, its unit adsorption amount was measured.

RESULTS AND DISCUSSION

1. Characterization of Materials

1-1. Determination of Isoelectric Point

To understand the electrical properties of the surface on D751-

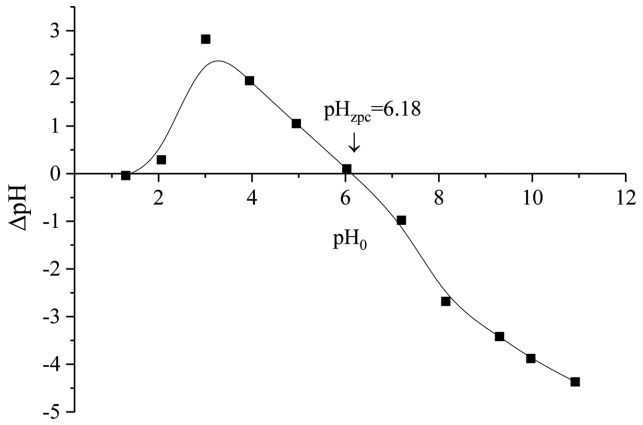

Fig. 1. Isoelectric point of D751-La.

La, an isoelectric point test was carried out (see Fig. 1).

It was shown that the isoelectric point about D751-La was 6.18. When the value of solution pH was lower than the pH_{pzc}, the surface of D751-La displayed positively charged; in turn, it showed negatively charged. The positive charge content of the surface on D751-La was highest under pH=3. It just explained that why the adsorption effect of phosphate was better at pH=3.

1-2. FTIR Analysis

For the purpose of judging the variance of the surface functional group above the material, the resin after adsorption of phosphate D751-La-P, D751-La and D751-Na were analyzed by FTIR scanning (see Fig. 2).

The absorption peaks at 1,015 and 1,120 cm^{-1} belonged to the stretching vibration peak with respect to the tertiary amine. After the modification, the peak was obviously weakened. It might be that the forming of coordination bond between the N on the tertiary amine and La reduced the amount of the tertiary amine. The absorption peak at 1,250 and 900 cm^{-1} should be due to the vibration absorption peak about the carboxylate, and the peak shape after modification was also weakened. It could be classified to the formation of a coordination bond between La and O on the C-O bond in the carboxyl group. Compared with the map of D751-Na, D751-La spectral showed a small absorption peak at 610 cm^{-1}; it should

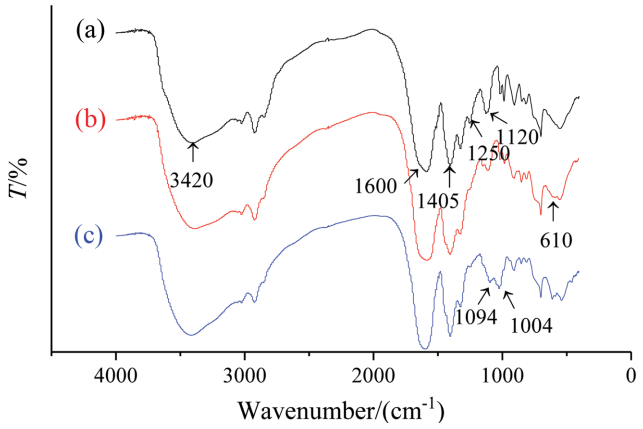

Fig. 2. FTIR spectra of D751-Na (a), D751-La (b) and D751-La-P (c).

be due to the stretching vibration peak of La-OH [17]. It indicates that La was successfully loaded onto the resin. D751-La-P showed a strong absorption peak at 1,094 and 1,004 cm^{-1}; it was part of the antisymmetric stretching vibration about PO_4^{3-} [18,19]. Luo et al. pointed out that the absorption peak at 1,037 cm^{-1} belonged the asymmetric vibration about P-O [20]. Fang et al. studied the mechanism of phosphate removal by barium hydroxide nanorods, indicating that typical P-O fingerprint characteristics were easily found in the range of 900 to 1,200 cm^{-1} [21]. These studies are identical to the FTIR characterization results of this study, indicating that D751-La can effectively adsorb phosphate.

1-3. SEM Analysis

To understand the change on surface morphology of D751-Na and D751-La (mainly by comparing surface particle size and uniformity), they were scanned by SEM. The scanning results are as follows. The surface on D751-Na was a random microporous granular structure with large and uneven particles (in Fig. 3(a)); however, the microporous particles on the surface of D751-La were arranged tightly, the particles were small, and the uniformity was also enhanced (in Fig. 3(b)). It demonstrated that there were certain differences in properties between D751-Na and D751-La.

1-4. XPS Analysis

To further judge the adsorption form of D751-La on phosphate,

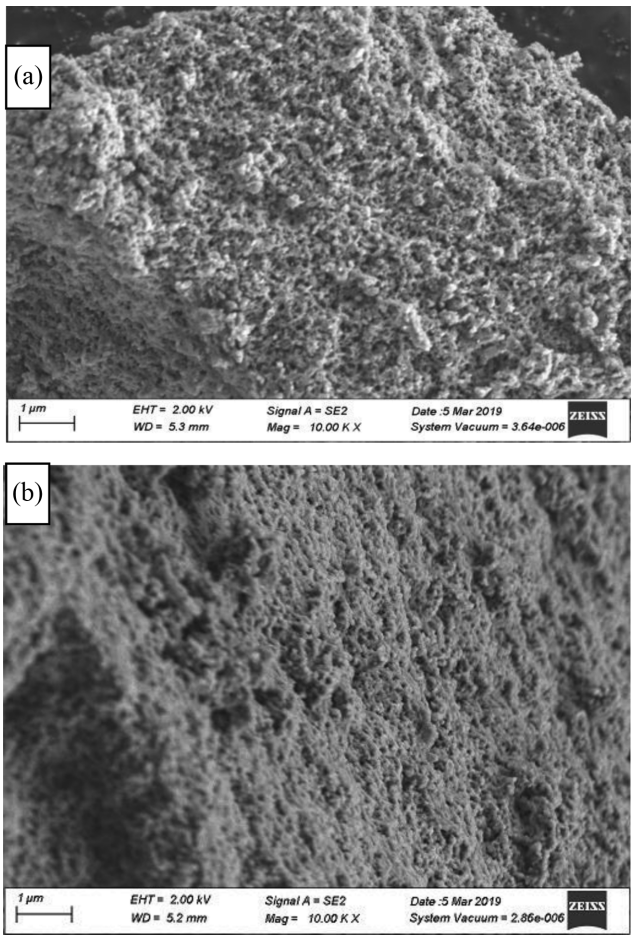

Fig. 3. SEM images of D751-Na (a) and D751-La (b).

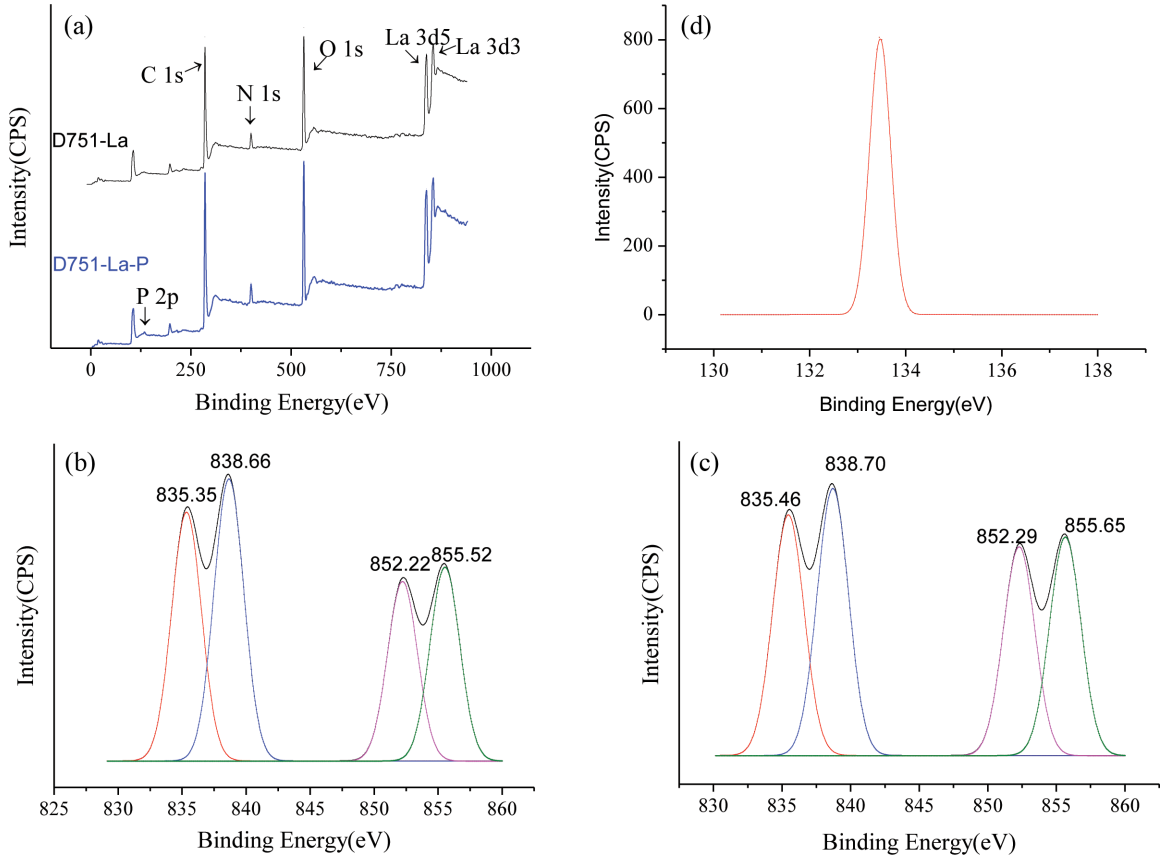

Fig. 4. (a) Full spectrum of XPS before and after adsorption of phosphate; (b) high resolution XPS spectrum of La 2p before adsorption of phosphate; (c) high resolution XPS spectrum of La 2p after adsorption of phosphate; (d) high resolution XPS spectrum of P 2p after adsorption of phosphate.

XPS analysis of the adsorbent before and after adsorption was carried out (charge correction was performed using standard C and Shirley background adjustment was used on the spectra), and some of the elements were peaked. The results are shown in Fig. 4. The total spectra before adsorption had absorption peaks at 284.8 eV, 400 eV, 533.1 eV, 838 eV and 855 eV, corresponding to C1s, N1s, O1s, La3d$_{3/2}$ and La3d$_{5/2}$, respectively. In contrast, the spectra of D751-La-P showed a split-new absorption peak located at 133 eV, which could be due to P2p [22]. It indicates that D751-La successfully adsorbed phosphate. It could be seen from the peak diagram of La before adsorption that 835.35 and 838.66 eV are La3d$_{3/2}$; 852.22 and 855.52 are La3d$_{5/2}$; the peak areas were 27.50%, 31.20%, 19.86% and 21.44%, respectively. After the adsorption of phosphate, the four peaks were shifted to 835.46, 838.70, 852.29, and 855.65 eV, while the peak area also changed, which was 25.73%, 28.56%, 22.34%, and 23.37%, respectively. This may be due to the La-O bond combining energy enhancements after phosphate adsorption [16,23]. From the peak of P at 133.47 eV, it could be seen that phosphate existed in the form of La-O-P(OH)$_3$, which is consistent with the results of infrared analysis.

2. Adsorption Studies

2-1. The Effect of pH

The solution pH has always played an extremely important role which often affects the adsorption performance of many adsorbents, while existing form of adsorbate was also affected in the adsorption process. Therefore, this study explored the function of the solution pH on the changing trend about the unit adsorption quantity toward phosphate by D751-Na and D751-La. Fig. 5 shows that the D751-Na had no adsorption ability, and the adsorption performance of D751-La toward phosphate was obviously improved.

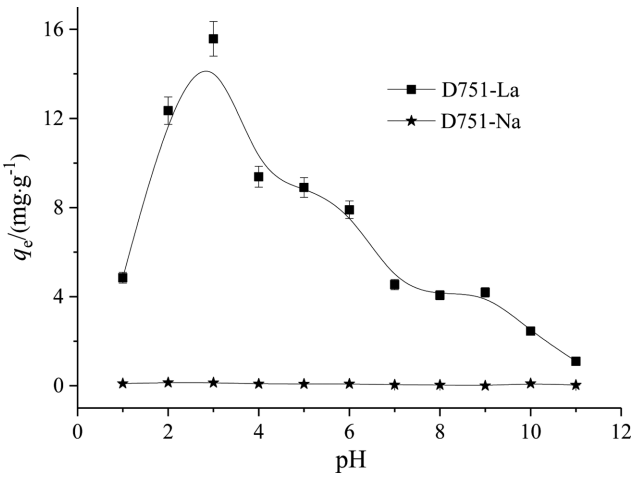

Fig. 5. Effect of pH on phosphate adsorption.

The value of q_e about phosphate adsorption onto D751-La increased rapidly with the increase of pH values from 1 to 3. The adsorption quantity, however, decreased rapidly as the pH increased progressively from 3 to 11.

The adsorption of phosphate was favorable under acidic conditions, especially at pH of 3. Similar results were obtained from other studies. For example, Liu et al., in the study of selecting adsorption of phosphate by using a new material of magnetic zirconium-based metal-organic frameworks, indicated that the adsorption was optimal as the solution pH=3 within the pH range tested [24]. Qiao et al. applied a new magnetic material to remove phosphate, pointing out that the magnetic Fe_3O_4/Zn-Al-Fe-La-LDH had the best adsorption capability of P in water at a pH of 4 [25]. In another study of phosphorus adsorption onto magenetic La and Ce-bimetal oxide shell, Han et al. showed that the adsorption toward phosphate was best at solution pH=3.0 [10]. The possible reasons for this trend were as follows: (1) phosphate was mainly present in the form of dihydrogen phosphate under acidic conditions, and the form was easily adsorbed by D751-La; (2) the surface positive charge of D751-La as the solution pH<6.18 got easy to be combined with negatively charged phosphate; (3) there was competitive adsorption between phosphate and OH^- in the solution with the acidity decreased [26]. Therefore, the adsorption of phosphate by D751-La showed a tendency that acidic conditions were better than alkaline conditions. In the human living environment, there are also many acidic phosphorus-containing wastewaters, such as phosphorus-containing wastewater from the phosphorus compound fertilizer processing industry and high-phosphorus wastewater from marine oil and gas pipeline cleaning [27]. Considering the practical application and the utilization of the adsorbent, the pH of the solution was chosen to be 3.0 and used for subsequent studies.

2-2. Effect of Adsorbent Dose

To ensure the utilization of the adsorbent, this experiment explored the effect of the dosage of D751-La on the action of phosphate. The results are presented in Fig. 6. The removal rate of phosphate, first of all, increased fast; soon after, tended to balance as the adsorbent dosage became large, while the unit adsorption amount gradually decreased (in Fig. 6). The reason could be attributed to that relatively more protons could be combined with the low amount

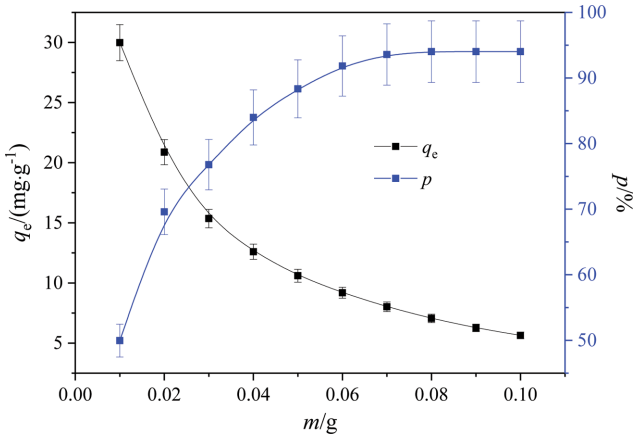

Fig. 6. Effect of the amount of adsorbent on phosphate adsorption.

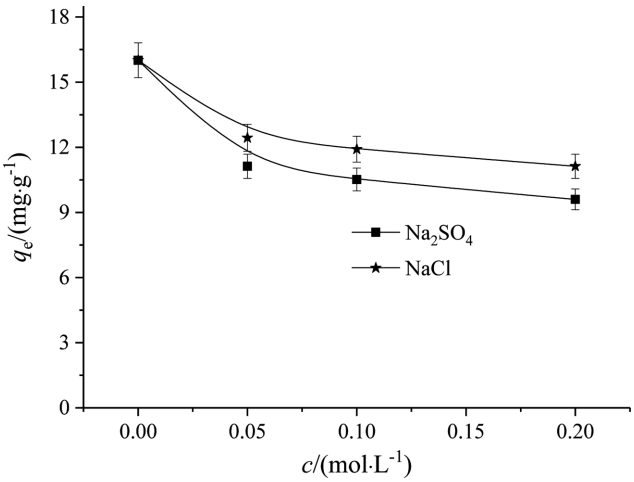

Fig. 7. Effect of salinity on phosphate adsorption.

of adsorbent, resulting in a larger amount of unit adsorption, and the active sites which located in the surface of D751-La were limited, resulting in a low removal rate of phosphate. The amount of relatively bound protons decreased with D751-La increased, so the unit adsorption amount was small, while the removal rate showed the trend: increased with the active sites increased on D751-La. When the adsorbent mass was 0.1 g, the removal rate was as high as 94% or more. The adsorbent mass was chosen to be 0.03 g for subsequent studies in consideration of the utilization of the adsorbent.

2-3. The Effect of Salinity

The influence of system salinity during adsorption is not negligible. For investigating the effect of salinity, this experiment explored the effect of two salts (NaCl and Na_2SO_4). The results are in Fig. 7. It was found that there was slight negative effect of common salts on adsorption quantity (in Fig. 7). The ion of SO_4^{2-}, compared with Cl^-, had a slightly greater influence for removing phosphate with the higher salt concentration, which might be the existence of competitive adsorption between SO_4^{2-} and phosphate. However, on the whole, the effect of salinity was not obvious for removing phosphate. Similar results were found on other phosphate adsorbents [28-30]. For example, Chen et al. used graphene-Lanthanum composite to selectively adsorb and efficiently remove phosphate, indicating that the composites for removing phosphate were more resistant to coexisting ions [29]. Gu et al. explored the removal of phosphate by zirconium loaded carbon nanotubes and found that there was no effect of salinity on phosphate adsorption [30]. It suggested that D751-La could be used to separate out phosphate from water with highly selectivity, and the effect of salinity could be ignored in subsequent experiments.

2-4. Adsorption Kinetics Study

For understanding the action process clearly, the effects of contact time on the adsorption quantity of phosphate by D751-La were investigated at three temperatures (see Fig. 8). It indicated that as the starting concentration of phosphate was constant, the unit adsorption amount of phosphate by D751-La, in the initial stage, increased rapidly, finally, became gently as the adsorption proceeded. It was due to there being more active sites located on the surface of D751-La at the beginning, the process was faster; the active sites

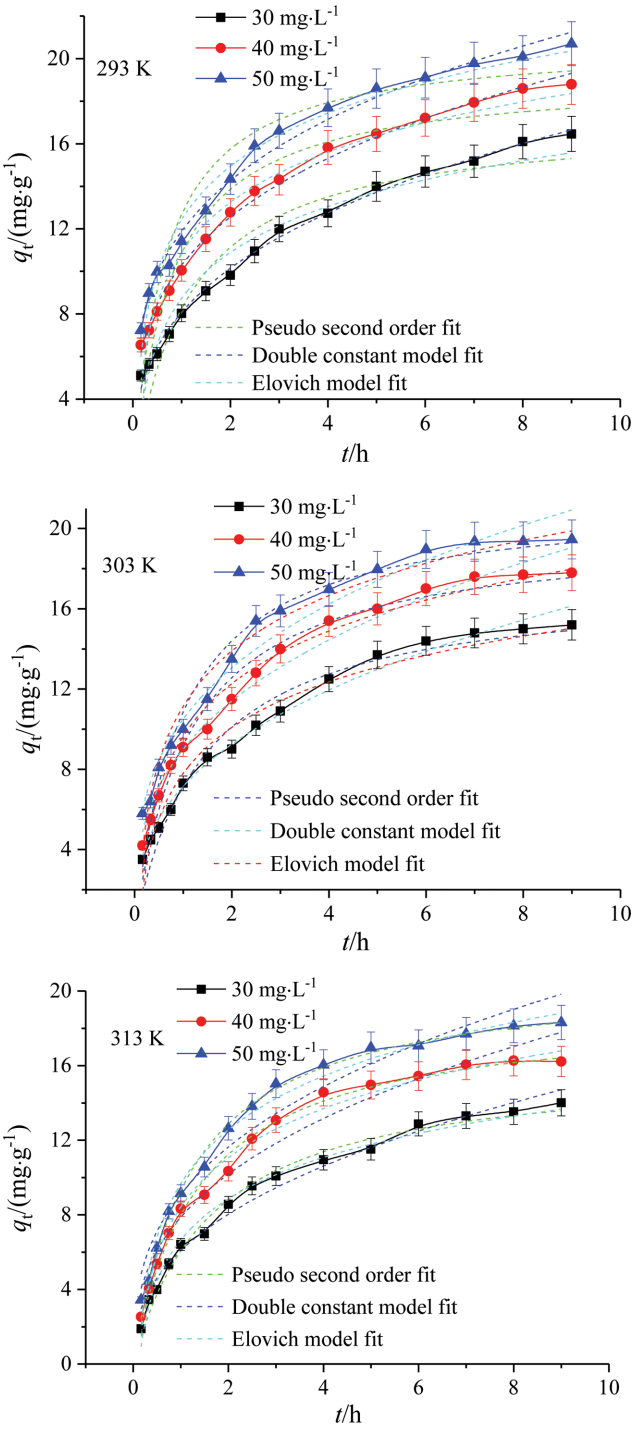

Fig. 8. Adsorption kinetics of phosphate adsorption onto D751-Fe.

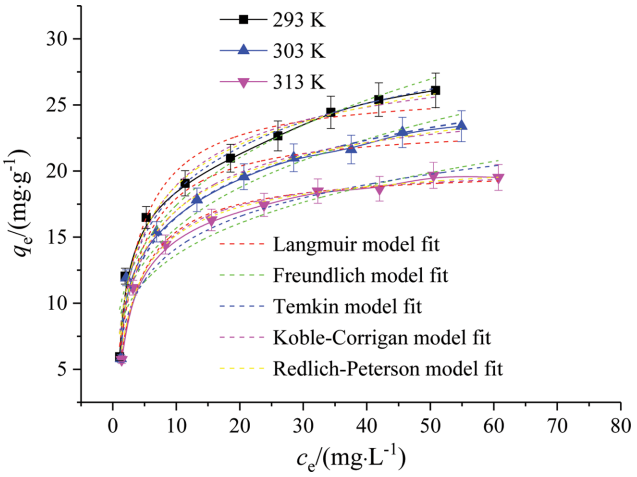

Fig. 9. Adsorption isotherms of phosphate adsorption onto D751-Fe.

decreased continuously with the adsorption progressed, then brought about the adsorption being slower. When the adsorption time was the same, the larger the initial concentration, the larger the unit adsorption quantity of D751-La resin for phosphate; it was because the number of active sites terminated on the same amount of D751-La; there were more protons that could be bound, and the unit adsorption amount was large in an equal time under the fierce competition for a phosphate solution with a large initial concentration.

Based on the purpose of exploring the adsorption mechanism between D751-La and phosphate, three kinetic models (listed in Table 1) were used to nonlinearly fit the adsorption process of phosphate by D751-La. The fitting results, corresponding parameters, as well as fitted curves are illustrated in Fig. 8 and Table 2, respectively.

Pseudo-second-order model (based on adsorption equilibrium quantity) is used to describe the adsorption process by chemical adsorption controlling rate [31]. Table 2 shows that the values of k_2 decreased with the temperature increased. This indicated that the reaction was classified an exothermic reaction. According to the larger determined coefficients ($R^2 \geq 0.909$) and the smaller error ($SSE \leq 24.0$), and the agreements of $q_{e(theo)}$ and $q_{e(exp)}$, the pseudo-second-order model could be taken out to depict the adsorption process, and in which there was chemical action [32]. Similar results could be found from other studies [29,33-36]. The Elovich model and Double Constant model can be used to describe the heterogeneous diffusion process. These data of large correlation coefficient $R^2 \geq 0.952$ and small $SSE \leq 16.1$ declared that the adsorption process could be well fitted by Double Constant and Elovich model, reflecting that there is physical adsorption among the uptake of phosphate. Overall, the adsorption process was a chemical-physical process.

2-5. Isothermal Adsorption Study

To further explore the adsorption property, this study explored the effect of temperature as well as balanced concentration on the adsorption of D751-La toward phosphate. The related results are demonstrated in Fig. 9. The unit adsorption amount, known from Fig. 9, increased at low levels of balanced concentration, and finally the increase rate slowed with the balanced concentration arise. In addition, the higher the adsorption temperature, the smaller the unit adsorption amount of the D751-La toward phosphate as the equilibrium concentration was persistent, reflecting that the process was exothermic. Moreover, the adsorption capacity of phosphate upon D751-La was as high as 26.3 $mg \cdot g^{-1}$.

For further explaining the reaction mechanism, the relationship between the unit adsorption amount and the adsorption concentration can be obtained at various temperatures from theory. By comparing with various isothermal adsorption models, five mod-

Table 1. Common adsorption models

Adsorption model	Nonlinear form	Symbol description
Isotherm model		
Langmuir model	$q_e=\frac{q_m K_L c_e}{1+K_L c_e}$	K_L is constant associated with binding energy ($L\cdot mg^{-1}$); q_m ($mg\cdot g^{-1}$) is monolayer theoretical saturated adsorption amount
Freundlich model	$q_e=K_F c_e^{1/n}$	K_F and 1/n are temperature dependent constants;
Temkin	$q_e=A+B\ln c_e$	A and B are equation parameters.
Koble-Corrigan model	$q_e=\frac{Ac_e^n}{1+Bc_e^n}$	A, B and n are equation parameters
Redlich-Peterson model	$q_e=\frac{Ac_e}{1+Bc_e^g}$	A, B and g are equation parameters
Kinetic model		
Pseudo-second-order kinetic model	$q_t=\frac{k_2 q_e^2 t}{1+k_2 q_e t}$	k_2 represents the pseudo-second-order rate constant ($g\cdot mg^{-1}\cdot min^{-1}$)
Double constant model	$\ln q_t=\ln A+K_s t$	K_s is the coefficient about adsorption rate, A is constant
Elovich model	$q_t=A+B\ln t$	A and B are constant

Table 2. Adsorption kinetics fitting parameters

Pseudo-second-order kinetic model						
T/K	$c_0/(mg\cdot L^{-1})$	$q_{e(exp)}/(mg\cdot g^{-1})$	$q_{e(theo)}/(mg\cdot g^{-1})$	$k_2/(g\cdot mg^{-1}\cdot min^{-1})$	R^2	SSE
293	30	16.5	17.1±0.9	0.0541±0.0123	0.911	17.9
	40	18.8	19.2±0.8	0.0678±0.0135	0.914	20.1
	50	20.7	20.8±0.8	0.0748±0.0146	0.909	24.0
303	30	15.2	17.3±0.6	0.0406±0.0067	0.964	8.03
	40	17.8	19.8±0.6	0.0438±0.0061	0.970	8.62
	50	19.5	21.4±0.7	0.0483±0.0074	0.959	13.3
313	30	14.0	16.1±0.4	0.0377±0.0040	0.988	2.54
	40	16.2	18.9±0.4	0.0387±0.0032	0.991	2.49
	50	18.3	20.8±0.3	0.0390±0.0026	0.994	2.12
Double constant equation						
T/K	$c_0/(mg\cdot L^{-1})$	$q_{e(exp)}/(mg\cdot g^{-1})$	A	K_s	R^2	SSE
293	30	16.5	8.08±0.10	0.329±0.007	0.995	1.02
	40	18.8	10.3±0.1	0.286±0.007	0.994	1.35
	50	20.7	11.9±0.2	0.265±0.009	0.988	3.06
303	30	15.2	7.15±0.16	0.370±0.014	0.987	2.86
	40	17.8	9.00±0.23	0.343±0.015	0.981	5.49
	50	19.5	10.5±0.3	0.314±0.017	0.972	9.10
313	30	14.0	6.08±0.20	0.402±0.019	0.980	4.14
	40	16.22	7.87±0.34	0.371±0.026	0.957	12.6
	50	18.3	9.10±0.40	0.355±0.026	0.953	16.1
Elovich equation						
T/K	$c_0/(mg\cdot L^{-1})$	$q_{e(exp)}/(mg\cdot g^{-1})$	A	B	R^2	SSE
293	30	16.5	8.73±0.26	3.11±0.19	0.952	9.64
	40	18.8	10.9±0.2	3.40±0.15	0.973	6.40
	50	20.7	12.4±0.2	3.61±0.15	0.977	6.09
303	30	15.2	7.80±0.22	3.29±0.16	0.967	7.27
	40	17.8	9.64±0.19	3.79±0.14	0.981	5.48
	50	19.5	11.1±0.2	3.98±0.18	0.972	8.73
313	30	14.1	6.65±0.15	3.20±0.11	0.985	3.13
	40	16.2	8.42±0.17	3.81±0.12	0.986	4.07
	50	18.3	9.67±0.18	4.16±0.13	0.986	4.94

Note: $SSE=\Sigma(q-q_c)^2$, q and q_c are the experimental value and calculated value according the model, respectively.

Table 3. Adsorption isotherm fitting parameters

Temkin				
T/K	A	B	R^2	SSE
293	7.37±0.72	4.81±0.26	0.978	7.13
303	6.78±0.82	4.22±0.28	0.965	8.30
313	6.12±0.75	3.49±0.25	0.960	5.95
Koble-Corrigan				
T/K	A	B	n	R^2	SSE
293	9.90±1.46	0.322±0.053	0.696±0.163	0.967	8.95
303	9.02±1.58	0.332±0.059	0.703±0.185	0.957	8.73
313	6.81±0.95	0.330±0.041	0.933±0.125	0.984	2.12
Redlich-Peterson				
T/K	A	B	g	R^2	SSE
293	0.778±0.404	13.0±4.2	0.879±0.055	0.975	6.90
303	0.726±0.425	11.3±4.1	0.891±0.061	0.963	7.47
313	0.422±0.124	7.36±1.20	0.961±0.036	0.986	1.82
Langmuir				
T/K	$K_L/(L\cdot mg^{-1})$	$q_{e(exp)}/(mg\cdot g^{-1})$	$q_{m(theo)}/(mg\cdot g^{-1})$	R^2	SSE
293	0.319±0.053	26.1	26.3±0.9	0.959	12.9
303	0.319±0.058	23.4	23.5±0.8	0.950	11.7
313	0.318±0.029	19.5	20.2±0.3	0.985	2.21
Freundlich				
T/K	K_F	1/n	R^2	SSE
293	9.32±0.92	0.271±0.029	0.939	19.2
303	8.67±0.91	0.257±0.031	0.925	17.5
313	7.99±0.89	0.233±0.033	0.901	14.8

els (also listed in Table 1) were chosen and used describe the process of removing phosphate by D751-La. The fitting results, relative data, and fitted curves are given in Fig. 9 and Table 3, respectively.

Langmuir model was selected to describe a single-layer uniform adsorption process in an ideal state [37]. Freundlich model is used to describe multi-layer non-uniform adsorption in a non-ideal state [38]. Compared with the two models, Langmuir had a larger $R^2\geq$ 0.950 and a smaller SSE≤12.9, as well as the high fit of $q_{e(theo)}$ (26.1 $mg\cdot g^{-1}$ at 293 K) and $q_{e(exp)}$ (26.3 $mg\cdot g^{-1}$ at 293 K), which made known that the adsorption process was a complex adsorption process with monolayer uniform adsorption being dominant, and multilayer non-uniform adsorption being supplemented. In addition, in the Freundlich model, the K_F value decreased with the temperature drop, intimating that the procedure of removing phosphate was an exothermic reaction [39].

Temkin model is commonly carried out to picture the form of non-uniform surfaces' adsorption. It was easy to find that Temkin model could be better describing the process about phosphate removal because of the high $R^2\geq0.960$ and the low SSE≤8.30. This implied that there was non-uniform surface adsorption in the adsorption process.

Koble-Corrigan model with three parameters is a combination of the two models: Langmuir and Freundlich [39]. It is seen from Table 3 that the n value tended to 1, indicating that the reaction tended to be described by the Langmuir model [38]. In addition, there was a high $R^2\geq0.957$ and a low SSE≤8.95, showing that the process of removing phosphate by D751-La could be better fitted by Koble-Corrigan model. It was further referred that there was uniform surface monolayer adsorption in the adsorption process.

Redlich-Peterson model is very good for the process in which uniform or non-uniform adsorption coexists. The parameter g with the range of 0-1 mirrors the extent of heterogeneity, the model is biased toward the Langmuir model as the value of g tends to 1 [40]. Table 3 shows that A and B were smaller with increasing temperature, indicating that the temperature increase was adverse to remove phosphate, and there were larger determined coefficients ($R^2\geq0.963$) and a smaller error (SSE≤7.47), indicating that Redlich-Peterson model was suitable for describing the complex diversity of the process. Overall, it reflected that there were single layer uniform adsorption and multiple layers of non-uniform adsorption in the process of removing phosphate.

2-6. Adsorption Thermodynamics

The direction of the reaction and whether the reaction reaches equilibrium, in the adsorption process can be revealed by knowing the change of energy. In practice, it can be judged by ΔG, ΔH, as well as, ΔS. The adsorption of phosphate by D751-La is an adsorption equilibrium process. The equilibrium constant ($K_c^{'}$) of adsorption process for removing phosphate by D751-La can be ob-

tained according to the following formula (3).

$$K_c^{'}=c_{ad,e}/c_e \quad (3)$$

Among them, c_e and $c_{ad,e}$ are the concentration of phosphate on D751-La as well as in the solution when the adsorption is balanced, respectively.

Calculating $K_c^{'}$ and bringing it into (4) to get the ΔG^0 value:

$$\Delta G^0=-RT\ln K_c^{'} \quad (4)$$

Here, ΔG^0 is the Gibbs free energy (J); T is the absolute temperature (K); R is the gas constant (8.314 J·mol^{-1}·K^{-1}); $K_c^{'}$ is the adsorption equilibrium constant.

Linear regression of ΔG-T was carried out by Gibbs-Helmholtz's formula (5). ΔH and ΔS were obtained from the intercept and slope above the line, respectively. ΔH, ΔS can be regarded as a constant with there being a little influence of temperature.

$$\Delta G^0=\Delta H-T\Delta S \quad (5)$$

For the actual system, not only the possibility of reaction but also the reaction rate should be considered. It can be expressed by activation energy. The apparent activation energy can be obtained by bringing the most consistent kinetic adsorption model parameters into the Arrhenius Eq. (6).

$$\ln k=-\frac{E_a}{RT}+\ln A \quad (6)$$

where k is a rate constant, E_a is the apparent activation energy (kJ·mol^{-1}), while A is the temperature influence factor.

Based on the formulas (4)-(6), the relevant thermodynamic parameters were acquired, as shown in Table 4.

ΔG^0 is used to judge the feasibility of the reaction. The negative ΔG revealed that the action of D751-La and phosphate was a spontaneous process. The negative ΔH demonstrated that the reaction belonged to an exothermic reaction, and ΔH (ΔH=−17.8 kJ·mol^{-1}) was far from the chemisorption of ruthenium (40-120 kJ·mol^{-1}), indicating that there was strong physical adsorption between D751-La and phosphate [38,40]. The negative ΔS indicated that phosphate moved from solution to the surface of D751-La during the adsorption process, and this made the degree of disorder decrease. This parameter E_a is often used to judge the form of adsorption. The negative E_a explained that the removal of phosphate by D751-La was exothermic and E_a (E_a=−13.8 kJ·mol^{-1}) deviated far from the range of 5-40 kJ·mol^{-1}, showed the presence of chemisorption between D751-La and phosphate [41]. In summary, the adsorption reaction was a spontaneous, entropic reduced exothermic reaction. Chemical adsorption and physical adsorption coexisted.

2-7. Adsorption Mechanism

This experiment shows that D751-La had a good adsorption effect on phosphate. However, D751-Na did not adsorb phosphate; it indicated that the La on D751-La acted on phosphate. Moreover, the effect be good under the solution of pH=3, which be attributed to electrostatic attraction, and the phosphate was mainly present in the form of $H_2PO_4^-$ and HPO_4^{2-} in the range of pH 3-11 [42,43]. Furthermore, the adsorption process was essentially unaffected by salinity, indicating that La on D751-La could form a complex with phosphate. Results of FTIR analysis and XPS analysis also showed that the action of phosphate and D751-La was in the form of La-$OP(OH)_3$. In summary, it be speculated that the reaction mechanism was a combination of physical adsorption (electrostatic attraction) and chemisorption (coordination reaction) between D751-La and phosphate [39]. The mechanism of action between D751-La and phosphate is shown in Fig. 10.

CONCLUSION

The adsorption capacity of D751 modified by $LaCl_3$ was clearly improved after La modification. It was in favor of adsorption at acidic condition. The isotherm fitting consequent manifested that the adsorption could be seen as a complex process: multi-layer non-uniform adsorption as well as single-layer uniform adsorption coexisted. The results of kinetic fitting revealed that the adsorption not only had chemical adsorption but also contained physical adsorption. Thermodynamic parameters showed that the adsorption reaction belonged to a spontaneous, entropic reduction exothermic reaction. Overall, D751-La has the potential to remove phosphate from water bodies.

ACKNOWLEDGEMENT

This work was supported in part by the Key Scientific Research

Table 4. Thermodynamic parameters

E_a (kJ·mol^{-1})	ΔH^0 (kJ·mol^{-1})	ΔS^0 (J·mol^{-1}·K^{-1})	ΔG^0 (kJ·mol^{-1})		
			293K	303K	313K
−13.84	−17.8	−53.2	−2.24	−1.77	−1.18

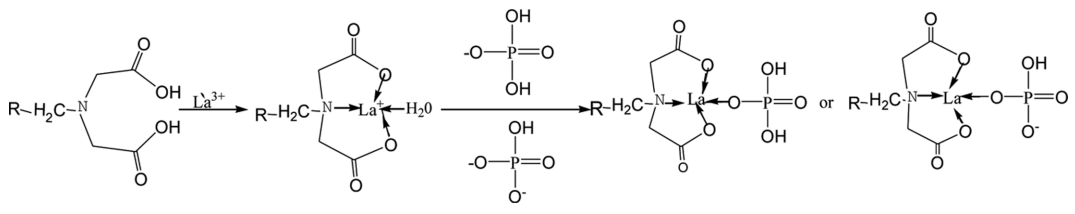

Fig. 10. Adsorption mechanism.

Project in Universities of Henan Province (19A150048).

REFERENCES

1. R. H. Li, J. L. Cui, X. D. Li and X. Y. Li, *Environ. Sci. Technol.*, **52**, 14119 (2018).
2. A. Othman, E. Dumitrescu, D. Andreescu and S. Andreescu, *ACS Sustain. Chem. Eng.*, **6**, 12542 (2018).
3. Y. Zhang, X. M. Guo, Y. Yao, F. Wu, C. Z. Zhang, R. J. Chen, J. Lu and K. Amine, *ACS Appl. Mater. Inter.*, **8**, 2905 (2016).
4. M. Kim, H. Kim and S. H. Byeon, *ACS Appl. Mater. Inter.*, **9**, 40461 (2017).
5. C. M. Nobile, M. N. Bravin, E. Tillard, T. Becquer and J. M. Paillat, *Soil Use Manage.*, **34**, 461 (2018).
6. Y. L. Zhang, H. Y. Ma, L. Lin, W. Z. Cao, T. Ouyang and Y. Y. Li, *ACS Sustain. Chem. Eng.*, **6**, 10989 (2018).
7. B. C. Pan, F. C. Han, G. Z. Nie, B. Wu, K. He and L. Lu, *Environ. Sci. Technol.*, **48**, 5101 (2014).
8. M. Amini, Z. A. Khoei and E. Erfanifar, *Biocat. Agricul. Biotechnol.*, **19**, 101097 (2019).
9. M. N. Afridi, W. H. Lee and J. O. Kim, *Environ. Res.*, **171**, 428 (2019).
10. M. Y. Han, J. H. Zhang, Y. Y. Hu and R. P. Han, *J. Chem. Eng. Data*, **64**, 3641 (2019).
11. J. Q. Zhu, J. Y. Li, Y. Y. Li, J. Guo, X. Yu, L. Peng, B. P. Han, Y. Zhu and Y. M. Zhang, *Sep. Purif. Technol.*, **223**, 196 (2019).
12. A. B. Savic, D. Cokesa, M. S. Bisercic, I. Castvan-Jankovic, R. Petrovic and L. S. Zivkovic, *Adv. Powder Technol.*, **30**, 1687 (2019).
13. J. J. Song, P. P. Huang, L. F. Chen, Z. W. Qi and J. G. Yu, *Chem. Ind. Eng. Progr.*, **31**, 370 (2012).
14. L. Dithme, A. S. Lipton, K. Reitzel, T. E. Warner, D. Lundberg and U. G. Nielsen, *Environ. Sci. Technol.*, **49**, 4559 (2015).
15. G. T. Adithya, S. Rangabhashiyam and C. Sivasankari, *Microchem. J.*, **148**, 364 (2019).
16. J. P. Hu, D. Z. Wu, R. L. Liu, R. Z. Rao and W. L. Lai, *J. Safety Environ.*, **16**, 237 (2016).
17. L. Chen, F. Liu, Y. Wu, L. M. Zhao, Y. Z. Li, X. Zhang and J. S. Qian, *Chem. Eng. J.*, **347**, 695 (2018).
18. H. H. Yi, Q. F. Yu, X. L. Tang, P. Ning, L. P. Yang, Z. Q. Ye and J. H. Song, *Ind. Eng. Chem. Res.*, **50**, 3960 (2011).
19. M. Saraf, P. Kumar, G. Kedawat, J. Dwivedi, S. A. Vithayathil, N. Jaiswal, B. A. Kaipparettu and B. K. Gupta, *Inorg. Chem.*, **54**, 2616 (2015).
20. X. B. Luo, X. Wu, Z. Reng, X. Y. Min, X. Xiao and J. M. Luo, *Ind. Eng. Chem. Res.*, **56**, 9419 (2017).
21. L. P. Fang, Q. T. Shi, J. Nguyen, B. L. Wu, Z. M. Wang and I. M. C. Lo, *Environ. Sci. Technol.*, **51**, 12377 (2017).
22. Z. C. Yang, L. H. Liu, L. Zhao, G. Su, Z. X. Wei, A. P. Tang and J. R. Xue, *J. Environ. Sci.*, **86**, 24 (2019).
23. D. Setyono and S. Valiyaveettil, *ACS Sustain. Chem. Eng.*, **2**, 2722 (2014).
24. T. Liu, S. R. Zheng and L. Y. Yang, *J. Colloid Interface Sci.*, **552**, 134 (2019).
25. W. C. Qiao, H. Bai, T. H. Tang, J. H. Miao and Q. W. Yang, *Colloids Surf. A*, **577**, 118 (2019).
26. X. Q. Li, J. Cui and Y. S. Pei, *J. Environ. Manage.*, **213**, 36 (2018).
27. Z. Y. Jia, Z. G. Wang, P. G. Cheng, Z. L. Xiang and N. Tang, *Water Treat. Technol.*, **40**, 83 (2014).
28. X. T. Zhang, R. Z. Zhang, S. S. Chen, K. Wen and R. P. Han, *Desalin. Water Treat.*, **170**, 187 (2019).
29. M. L. Chen, C. B. Huo, Y. K. Li and J. H. Wang, *ACS Sustain. Chem. Eng.*, **4**, 1296 (2016).
30. Y. F. Gu, M. M. Yang, W. L. Wang and R. P. Han, *J. Chem. Eng. Data*, **64**, 2849 (2019).
31. Y. C. Rong and R. P. Han, *Korean J. Chem. Eng.*, **36**, 942 (2019).
32. F. Z. Xie, Z. L. Dai, Y. R. Zhu, G. L. Li, H. B. Li, Z. Q. He, S. X. Geng and F. C. Wu, *Colloids Surf. A*, **562**, 16 (2018).
33. W. H. Zou, H. J. Bai and S. P. Gao, *J. Chem. Eng. Data*, **57**, 2792 (2012).
34. R. D. Zhang, J. H. Zhang, X. N. Zhang, C. C. Dou and R. P. Han, *J. Taiwan Inst. Chem. E.*, **45**, 2578 (2014).
35. J. Chen, L. G. Yan, H. Q. Yu, S. Li, L. L. Qin, G. Q. Liu, Y. F. Li and B. Du, *Chem. Eng. J.*, **287**, 162 (2016).
36. X. H. Liu, E. M. Zong, W. J. Hu, P. G. Song, J. F. Wang, Q. C. Liu, Z. Q. Ma and S. Y. Fu, *ACS Sustain. Chem. Eng.*, **7**, 758 (2019).
37. B. L. Zhao, W. Xiao, Y. Shang, H. M. Zhu and R. P. Han, *Arab. J. Chem.*, **10**, s359 (2017).
38. M. Y. Han, Q. Wang, H. Li, L. Y. Fang and R. P. Han, *Desalin. Water Treat.*, **115**, 271, (2018).
39. Y. F. Gu, M. Y. Liu, M. M. Yang, W. L. Wang, S. S. Zhang and R. P. Han, *Desalin. Water Treat.*, **138**, 368 (2019).
40. Y. Y. Hu and R. P. Han, *J. Chem. Eng. Data*, **64**, 791 (2019).
41. S. Chen, C. X. Qin, T. Wang, F. Y. Chen, X. L. Li, H. B. Hou and M. Zhou, *J. Mol. Liq.*, **285**, 62 (2019).
42. R. Xue, J. Xu, L. Gu, L. H. Pan and Q. He, *Water Air Soil Poll.*, **229**, 1 (2018).
43. X. Q. Li, J. Cui and Y. S. Pei, *J. Environ. Manage.*, **213**, 36 (2018).